# Retention of Iodide by Chloride Green Rust and Magnetite

Tim Platte,* Nicolas Finck,* Frank Heberling, Robert Polly, Tim Prüssmann, Kathy Dardenne, and Horst Geckeis

**ABSTRACT:** Green rust (GR), a layered double hydroxide (LDH) containing Fe, and magnetite can be found in natural and engineered environments. The ability of chloride GR (GR-Cl) and magnetite to retain iodide as a function of various parameters was investigated. Sorption equilibrium is achieved within 1 day of contact time between iodide and preformed GR-Cl in suspension. $pH_m$ variations (7.5−8.5) have no significant influence, but the iodide sorption decreases with increasing ionic strength set by NaCl. Sorption isotherms of iodide suggest that the uptake operates via ionic exchange (IC), which is supported by geochemical modeling. The short-range binding environment of iodide associated with GR is comparable to that of hydrated aqueous iodide ions in solution and is not affected by $pH_m$ or ionic strength. This finding hints at an electrostatic interaction with the Fe octahedral sheet, consistent with weak binding of charge balancing anions within an LDH interlayer. The presence of sulfate anions in significant amounts inhibits the iodide uptake due to recrystallization to a different crystal structure. Finally, the transformation of iodide-bearing GR-Cl into magnetite and ferrous hydroxide resulted in a quantitative release of iodide into the aqueous phase, suggesting that neither transformation product has an affinity for this anionic species.

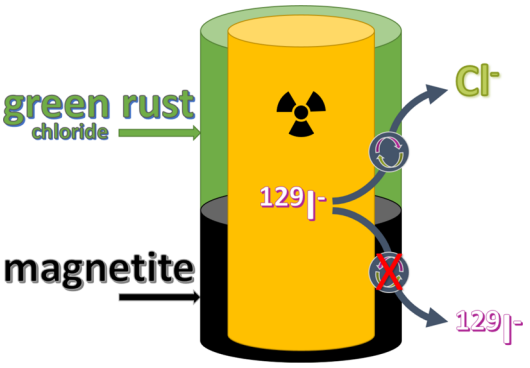


**KEYWORDS:** *Chloride green rust, Iodide, X-ray diffraction, X-ray absorption spectroscopy, nuclear waste disposal, magnetite, sorption*

## INTRODUCTION

Geological disposal is considered as the internationally preferred option to dispose of radioactive waste. In such repositories, the waste matrix is intended to be encapsulated in metallic containers and surrounded by engineered barriers. Canisters may start corroding when in contact with groundwater, resulting in the formation of Fe(II)-bearing phases such as green rust (GR) compounds,[1−3] which are known to be transient compounds between metallic iron and final, thermodynamically more stable corrosion products. GR is the Fe endmember of the layered double hydroxide (LDH) family and bears a permanent positive layer charge that is balanced by anions and water molecules in the interlayer. The general structural formula of GR can be written as $[Fe(II)_{1-x}Fe(III)_x(OH)_2]^{x+}$ $[(x/n)A^{n-}, mH_2O]^{x-}$, with $x$ representing the fraction of ferric iron and A representing the intercalated anions.[4] Depending on the nature of the intercalated anions, GR can crystallize either with a rhombohedral (e.g., chloride or carbonate green rust) or a hexagonal (e.g., sulfate green rust) unit cell. Because of the abundance of chloride ions in various groundwaters, chloride-containing GR (GR-Cl) should be considered as one possible phase occurring upon iron corrosion in suboxic and anoxic environments. These phases are especially expected in scenarios assuming corroding steel containers in a deep geological repository (DGR) in rock salt formations.[5−8] Depending on the anionic composition of the groundwater, carbonate- and sulfate-containing GR are also likely to be present.[9,10]

Anionic species intercalated within LDHs can be exchanged for negatively charged species present in the contacting solution. This mechanism gives these layered minerals the ability to bind dissolved anionic pollutants present in groundwaters which may otherwise be only poorly retained by clay minerals.[11,12] This ability to sorb anionic species can be of great interest, especially in the near-field of a DGR for nuclear waste. For example, nuclear waste contains significant amounts of long-lived $^{129}I$ (half-life of $1.57 \times 10^7$ years) which will be partially released as dissolved iodide species as soon as groundwater comes into contact with the waste matrix,[13] and which is hardly retained by major mineral phases in the near-field (e.g., clay minerals).[11,12,14−17] However, the mobility of anionic species such as iodide in aqueous environments may be lowered upon interaction with LDHs such as AFm phases in

cementitious material[18] and GR. The goal of this study is to investigate the iodide retention by preformed GR-Cl in suspension and to thoroughly characterize the involved uptake mechanism in order to establish a reliable geochemical model for potential iodide retention in the near-field.

The preparation of iodide-containing GR (GR-I) and of a complete solid solution between the isostructural iodide and chloride GR endmembers has been reported.[19,20] However, the concentrations of dissolved iodide used in these studies substantially exceed the amounts expected in the case of canister failure in a DGR. The aim of this study is to investigate the sorption behavior of iodide by preformed GR-Cl at different $pH_m$, contact times, and ionic strengths using more environmentally relevant iodide concentrations. Additionally, sorption experiments in the presence of sulfate have been performed where the porewater should be closer to real conditions as sulfate is naturally present in groundwaters. We also investigated the fate of iodide during conversion of iodide-bearing GR-Cl samples into magnetite and compared the results to those obtained in uptake experiments by preformed magnetite. Conversion reactions from iodide-bearing GR to the thermodynamically more stable magnetite aim to mimic reactions expected to occur during canister corrosion in a DGR over longer periods of time.

## MATERIALS AND METHODS

**Sample Preparation.** All samples have been prepared using ultrapure water (UPW, 18.2 MΩ·cm, Milli-Q system, Millipore) and reagents of ACS grade or higher. The sources of Fe(II), Fe(III), Cl(−I), $SO_4^{2-}$ and I(−I) were $FeCl_2{\cdot}4H_2O$, $FeCl_3$, NaCl, $Na_2SO_4$ and NaI, respectively. Unless otherwise indicated, all steps from sample preparation to analysis were performed under anoxic conditions by using an Ar-filled glovebox (<1 ppm of $O_2$) and airtight transfer vessels and sample holders. The NaOH solution was likewise prepared by dissolving NaOH(s) into degassed UPW in the glovebox. pH values were measured with a glass combination pH electrode (Metrohm LL Solitrode) that was calibrated before each use by commercial pH buffer solutions (pH 4, 7, 10). For samples at high ionic strength, the measured operational "pH" values have been corrected to $pH_m$ according to the literature.[21] Redox potentials (or $E_h$ values) were recorded using a combined platinum electrode (Radiometer Analytical); all reported values are quoted with respect to the standard hydrogen electrode. Suspensions were stirred during $E_h$ and $pH_m$ measurements. With respect to samples at high salinity, molality was used as the unit of concentration ($a_i \neq c_i$). At ionic strengths below 0.1 mol/L, the conversion shows no significant difference (mol/L ≈ mol/kg).

GR and magnetite samples have been prepared by titrating a stirred solution containing Fe(II) and Fe(III) with a 1 M NaOH solution until $pH_m$ 7.5 (GR, Fe(II)/Fe(III) = 4:1) or 9.5 (magnetite, Fe(II)/Fe(III) = 1:2). Although the Fe(II)/Fe(III) ratio in GR-Cl is close to 3,[19] a slightly higher ratio was used to prevent the formation of magnetite and to favor the GR formation.[22] After aging for 1 day, the suspension was first washed by centrifuging for 10 min at 3,500 rpm (2,000$g$) and replacing the supernatant by UPW. For centrifugation only, the sample was taken out of the glovebox in vials sealed with Parafilm. Suspensions were subsequently used in uptake experiments (9 ± 2 g/kg for GR, 6.9 ± 1.5 g/kg for magnetite). For each individual sorption sample the ionic strength was set by adding NaCl powder and the $pH_m$ was adjusted by using 1 M NaOH or 1 M HCl. Iodide was added and each sample was spiked with $^{125}I$ (100−300 Bq/mL) to quantify the uptake using gamma spectrometry.

The effect of several parameters on the iodide sorption by GR was investigated. In all cases, replicates were prepared and sampled after various contact times. Results showed that after 1 day there was no significant change in the sorption values. Investigated parameters were the ionic strength set by NaCl and adjusted to 0.2−5 M, the $pH_m$ adjusted within the range 7.0−8.5 for GR and 8.0−10.0 for magnetite, and the starting iodide concentration. After 2 weeks of contact time, a fraction of some of the GR sorption samples was converted into magnetite by titrating with 1 M NaOH to $pH_m$ 11.0.[23] This conversion was completed after 10 days. The complete sample list considered in this study can be found in Table S1 in the Supporting Information.

For the analysis of the samples, suspensions were ultracentrifuged for 60 min at 90,000 rpm (Beckman Coulter XL-90K), the concentration of iodide in the supernatant was quantified using a $\gamma$-counter (Packard Cobra Auto-Gamma 5003), and the concentration of dissolved Fe was quantified by ICP-MS (Thermo Scientific Element XR). The precise quantity of suspended solid phase was determined considering the total mass balance of Fe in the system and results from ICP-MS analysis. These exact values were taken into account to calculate the sorption coefficient $R_d$ as

$$R_d\left[\frac{\text{kg}}{\text{g}}\right] = \left(\frac{c_0 - c_L}{c_L}\right) \times \frac{m_j[\text{kg}]}{m[\text{g}]} \quad (1)$$

where $c_0$ is the initial iodide concentration, $c_L$ is the iodide concentration at equilibrium, $m_j$ is the mass of the solvent, and $m$ is the mass of the solid phase. Since molality was used as the unit of concentration in the manuscript, this is also taken into account in the sorption coefficient $R_d$ by using the mass of water (kg $H_2O$) instead of its volume (L).

**Solid Phase Characterization and X-ray Absorption Spectroscopy.** For the analysis of GR and magnetite compounds (XRD (X-ray diffraction), SEM-EDX (scanning electron microscopy and energy-dispersive X-ray spectroscopy), and XAS (X-ray absorption spectroscopy)), an aliquot of the sample slurry was centrifuged in the glovebox at 13,000 rpm (14,000$g$) for 15 min. The supernatant was removed and replaced by UPW twice. For XRD analysis the sample was encapsulated in an airtight and low background holder equipped with an O-ring. Diffractograms have been recorded using a D8 ADVANCE diffractometer equipped with a Cu anode and a LynxEye XE-T detector (Bruker AXS). Identification of the crystalline phase was performed by comparison with the PDF-2 database using DIFFRAC.EVA v5.0 (Bruker AXS). For SEM analysis, a small amount of slurry was dried on a sample holder, which was transported to the microscope [Quanta 650 FEG (FEI)] under anoxic conditions and placed into the microscope quickly to minimize air exposure as much as possible.

Information on the iodine short-range coordination environment was provided by XAS at the iodine K-edge. X-ray absorption spectra were recorded at room temperature at the ACT station of the CAT-ACT beamline[24] at the KIT light source (Karlsruhe Institute of Technology, Germany) with a storage ring energy of 2.5 GeV. Detailed information on sample preparation, experimental setup, and data treatment

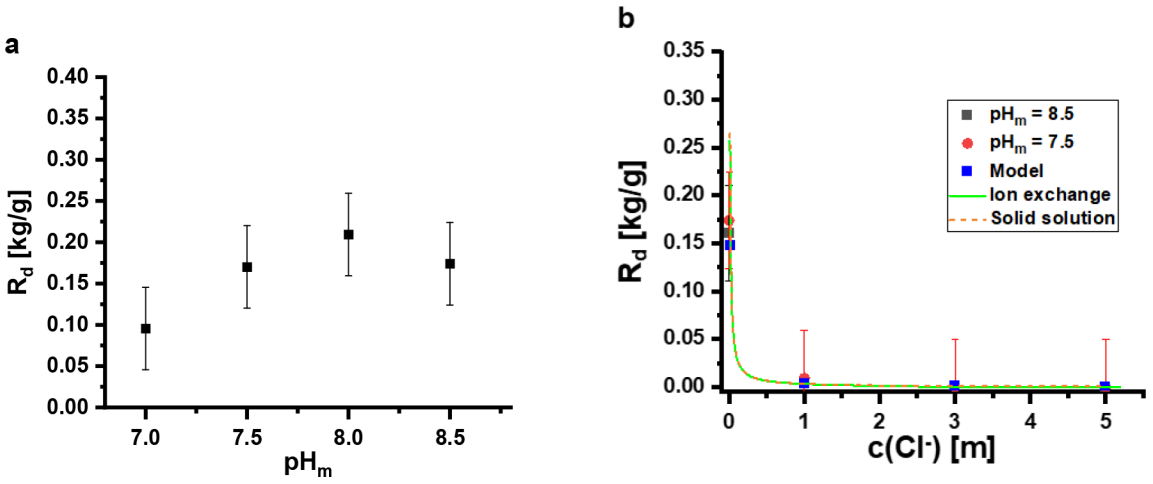


**Figure 1.** Sorption of iodide by GR-Cl as a function of $pH_m$ (a). Sorption of iodide by GR-Cl at different NaCl concentrations (b). Data correspond to averaged values between 1 and 7 days. Equilibrium was reached within 1 day. Blue squares show the model calculation, at the exact experimental conditions, as they were applied for the adjustment of the ion-exchange parameter. The continuous lines represent generic model calculations at average experimental conditions: $pH_m$ 7.5, $c$(GR) = 9 g/kg, $c_0(I^-)$ = 15 $\mu$M. The experimental data and model agree well at all $c(Cl^-)$ up to 5 M.

following standard procedures can be found in the Supporting Information.

**Modeling of Sorption Data.** Geochemical modeling was performed using PHREEQC 3 and the thermodynamic database SIT.dat (PHREEQC Interactive v. 3.4.0-12927 SIT.dat database).[26] Two models were developed in order to analyze possible uptake mechanisms and to describe experimental results quantitatively, an ion-exchange model and a solid solution model. The ion-exchange model uses an affinity parameter for $I^-$ binding relative to $Cl^-$ binding to exchange sites ($GR^+$), and the latter uses only the GR-I solubility constant as an input parameter for the uptake calculations. The solid solution model is a thermodynamic, more complete description, while the exchange model does not take solid phase stability and solubility into account. To model the ion-exchange reaction, two half-reactions were defined (eqs 2 and 3), which sum up to the overall ion-exchange process (eq 4).[25] The overall affinity of iodide to exchange for chloride in the GR structure, $\log(k_s)$ as defined by eq 5, was adjusted to obtain an optimal fit between data and model.[27] The individual constants for the half-reactions (eqs 2 and 3) are arbitrary (i.e., one is defined relative to the other):

$$GR^+ + I^- \rightleftarrows \text{GR-I}, \quad \log(K_I) \tag{2}$$

$$GR^+ + Cl^- \rightleftarrows \text{GR-Cl}, \quad \log(K_{Cl}) \tag{3}$$

$$\text{GR-Cl} + I^- \rightleftarrows \text{GR-I} + Cl^-, \quad \log\left(\frac{K_I}{K_{Cl}}\right) \tag{4}$$

$$\log(k_s) = \log\left(\frac{K_I}{K_{Cl}}\right) \tag{5}$$

As an alternative model, the iodide uptake by GR-Cl has been described as a solid solution between GR-Cl ($Fe(II)_3Fe(III)(OH)_8Cl{\cdot}nH_2O$) and GR-I ($Fe(II)_3Fe(III)(OH)_8I{\cdot}nH_2O$).[28] For this purpose, the solubility of GR-Cl was recalculated from the reported free energy formation ($dG$ = −2131.75 kJ/mol[29]) as $\log K_{SP}$(GR-Cl) = −79.70 (eq 6). The unknown solubility of GR-I was taken as an adjustable parameter.

$$\log(K_{SP}(\text{GR-Cl})) = 1.0a(Fe^{3+}) + 3.0a(Fe^{2+}) + 8.0a(OH^-) + 1.0a(Cl^-) \tag{6}$$

## RESULTS AND DISCUSSION

**Characterization of GR and Magnetite.** X-ray diffractograms of the synthesized GR compounds (Figure S1) evidence the presence of only green rust minerals, and electron micrographs show that samples are made of thin hexagonal platelets (Figure S3). These results compare well with reported findings for GR-Cl samples prepared by precipitation from ferric and ferrous ions or by oxidation of $Fe(OH)_2$.[19,23] The synthesized magnetite is made of octahedral crystals of 100−200 nm, and the crystal structure was assessed by XRD analysis (Figures S2 and S4).

**Iodide Sorption by GR-Cl.** The sorption of iodide by GR-Cl is only slightly affected by $pH_m$ variations (Figure 1). Results show a constant sorption with an adsorption coefficient $R_d$ of 0.18 ± 0.05 kg/g in the $pH_m$ range of 7.5−8.5, which slightly decreases to $R_d$ = 0.10 ± 0.05 kg/g at $pH_m$ 7. Since variations are within uncertainties, results evidence that $pH_m$ does not play a significant role on iodide adsorption. Note that GR is stable only in a limited pH range.[30] In contrast, the $Cl^-$ concentration has a significant influence on the iodide sorption. $R_d$ decreases from 0.17 ± 0.05 kg/g in 0.02 M NaCl to ∼0 in ≥1 M NaCl (Figure 1) at $pH_m$ 7.5, and comparable results were also obtained at $pH_m$ = 8.5. This dependency of the iodide sorption on the $Cl^-$ concentration is consistent with sorption studies of iodide on GR-Cl by Min et al.[31] Results further agree with sorption studies on other LDH phases (i.e., the absence of pH effect on iodide uptake by LDH)[32] and conform to expectations, since according to eq (4) the ion-exchange mechanism is independent of the $pH_m$ but strongly dependent on the $Cl^-$ concentration.

The next varied parameter was the starting iodide concentration at a constant solid/liquid ratio and at two $pH_m$ values. The adsorption isotherm and $R_d$ values are shown

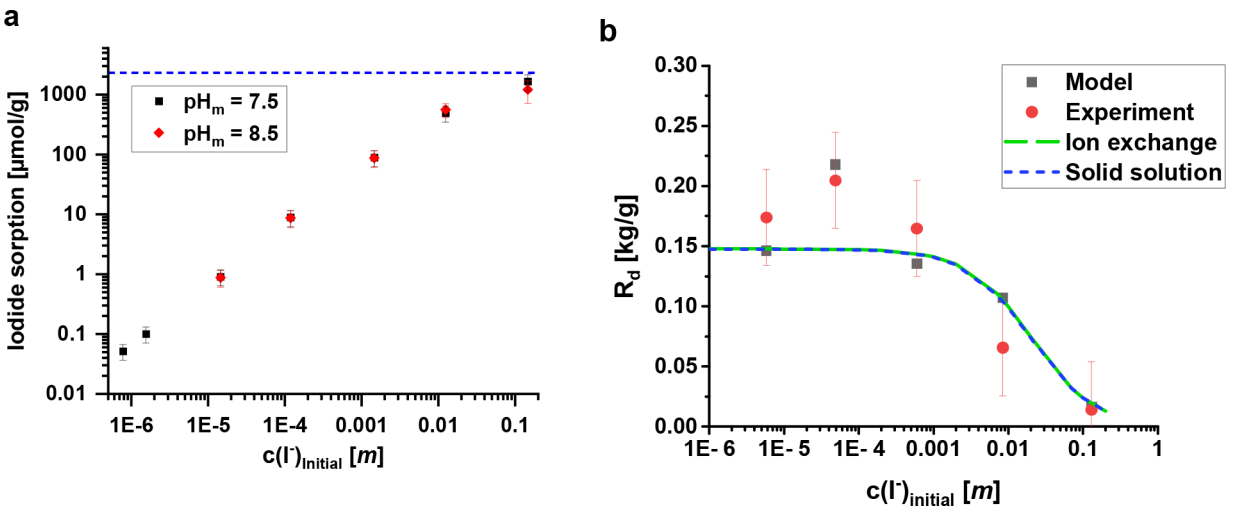


**Figure 2.** (a) Adsorption isotherms for the sorption of iodide by GR-Cl at different iodide concentrations. $c$(GR) ≈ 9 ± 2 g/kg, $c$($Cl^-$) ≈ 0.02 ± 0.01 M. The uncertainty on the iodide concentration is given in Table S2. The maximum amount of anion-exchange sites of GR-Cl is indicated by a blue dashed line in graph (a). (b) $R_d$ values at $pH_m$ 7.5. Black squares show the model calculation, at the exact experimental conditions, as they were applied for the adjustment of the ion-exchange parameter. The continuous lines represent generic model calculations at average experimental conditions: $pH_m$ 7.5, $c$(GR) = 9 g/kg, $c_0$(NaCl) = 0.02 mM.

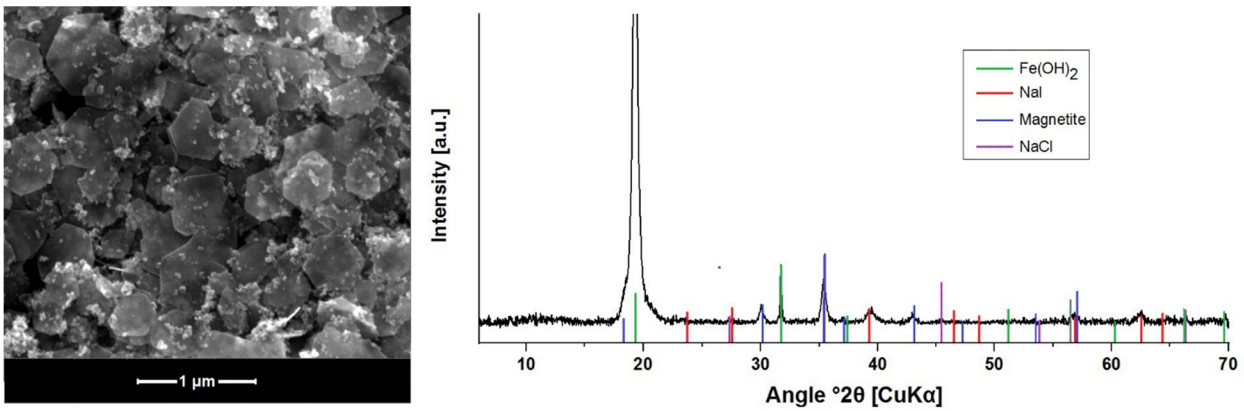


**Figure 3.** Scanning electron micrograph (left) and X-ray diffractogram (right) of a GR-Cl sorption sample converted into magnetite and $Fe(OH)_{2(s)}$ by adding NaOH. $pH_m$ = 11 ± 1, $c$($Cl^-$) = 0.02 ± 0.02 M. On the diffractogram vertical lines show the reference reflections of magnetite,[37] $Fe(OH)_2$,[38] NaI,[39] and NaCl.[39]

in Figure 2; $R_d$ values are further listed in Table S2. The double logarithmic adsorption isotherm shows a fairly linear increase of adsorption with increasing concentration, in line with anionic exchange as the sole sorption mechanism. At starting iodide concentrations ≥0.15 M, the slope of the adsorption isotherms, and thus the $R_d$ values, decreases. Comparable observations have been reported recently by Nedyalkova et al.,[33] who interpreted this behavior as a saturation of the uptake sites. Indeed, data and models indicate iodide concentrations in the solid become high relative to the concentration of available exchange sites at these aqueous concentrations. The change of $pH_m$ only marginally affects the sorption. It was attempted to record an adsorption isotherm at high ionic strength (5 M), but sorption was below the detection limit at these conditions.

**Iodide Sorption by Magnetite.** Iodide batch sorption experiments have been performed with magnetite at various $pH_m$ values and ionic strengths (Tables S1 and S4). After 7 days of contact time, the iodide sorption was below the limit of analytical uncertainty. Varying the contact time, $pH_m$, or ionic strength had no effect on the uptake. Separately, magnetite was also prepared in the presence of iodide (coprecipitation experiments). Using this approach, no significant iodide uptake could be detected either. The absence of a significant retention of iodide may be related to the development of a negative surface charge on magnetite under the considered $pH_m$ conditions, which hinders anions from binding the surface.[34] Furthermore, X-ray diffractograms showed no structural difference between magnetite synthesized in the absence of iodide, magnetite prepared in the presence of iodide, and magnetite after sorption with iodide.

**Transformation of GR-Cl Sorption Samples into Magnetite.** GR can be transformed into magnetite and $Fe(OH)_{2(s)}$[35] by increasing the $pH_m$ to >10. Table S3 shows precisely which samples have been used for transformation. Analysis by XRD of transformation samples (Figure 3) corroborated the presence of ferrous hydroxide and magnetite besides NaCl and NaI salts, as well as the absence of GR. Electron micrographs showed that $Fe(OH)_{2(s)}$ is present as large hexagonal platelets and magnetite as a fine-grained material, which agrees with earlier works.[23,35] The analysis of the supernatant further revealed that iodide is no longer bound

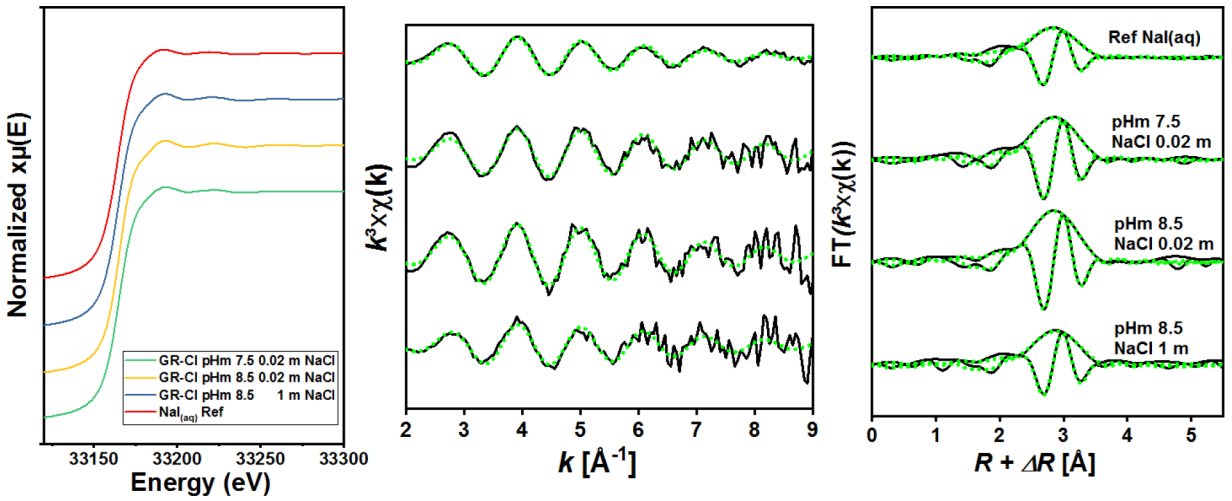


**Figure 4.** Iodine K-edge XANES of GR samples and the $NaI_{(aq)}$ reference (left). Experimental (solid black line) and modeled (dashed green line) EXAFS spectra (middle) with the corresponding Fourier transforms (right) of all samples. Fit results are presented in Table 1.

to any solid phase, meaning that iodide that was originally bound to GR has been released into solution during the transformation. This result implies that neither magnetite nor $Fe(OH)_{2(s)}$ are able to sorb iodide. Ferrous hydroxide has a layered structure; however, in contrast to GR, it does not bear any permanent layer charge, and its isoelectric point is at $pH_m$ about 10.[36] The absence of iodide retention by this compound in significant amounts can be related to either the absence of a permanent layer charge or to the development of a negative surface charge under the applied $pH_m$ conditions ($pH_m$ = 11). LDH compounds have two surface sites available for sorption, the planar sorption sites and the edge sites. The planar sites bear a permanent positive charge arising from the substitution of divalent by trivalent cations within the octahedral sheet, while edge sites consist of amphoteric hydroxyl surface functional groups (e.g., $\equiv Fe^{2+}-OH$ and $\equiv Fe^{3+}-OH$ for GR). Considering reported studies on other LDHs,[33] experimental findings may suggest that iodide anions can only occupy interlayer sites where they are held through electrostatic attraction and cannot sorb on edge sites. Magnetite has a point of zero charge of pH = 6.4.[34] At pH around 10, the surface thus has a negative surface charge, which could be one origin to the absence of iodide species retention by magnetite.

**Iodide Sorption by GR-Cl in the Presence of Sulfate.** The influence of the presence of sulfate in the sorption experiments with GR has also been investigated (see Tables S6 and S7). At low sulfate concentrations (1−32 $\mu$m, concentrations comparable to that of iodine), no significant influence on the iodide retention could be evidenced; calculated $R_d$ values are in the same range (≈0.18 kg/g) as that for sorption without added sulfate (≈0.17 kg/g). At higher sulfate concentrations (35−45 mM, concentrations comparable to that of chloride) the iodide retention significantly decreased, and the sorption constant $R_d$ is below the detection limit.

In the presence of sulfate, GR-Cl can transform into sulfate green rust (GR-$SO_4$) due to the higher stability of this latter compound.[40] Earlier studies showed that for 2.5 g/L GR-Cl (i.e., ∼6 mmol/L) and crystallite sizes comparable to that in the present study (Figure S3), ∼90% of the exchange sites are occupied by $SO_4^{2-}$ for aqueous solutions containing 40 mmol/L $Cl^-$ and 5 mmol/L $SO_4^{2-}$ ($SO_4^{2-}/Cl^-$ = 1:8).[41]

In experiments at low sulfate concentrations, the amount of formed GR-$SO_4$ is likely very low, i.e., the presence of 32 $\mu$mol/L sulfate and ∼20 mM NaCl in uptake experiments with 9 g/kg GR-Cl (i.e., ∼20 mmol/L GR-Cl) may have resulted in the transformation of <1% of GR-Cl into GR-$SO_4$. Experimental sorption data show that this low amount of GR-$SO_4$ has no significant effect on iodide uptake.

The uptake of iodide by GR-Cl works very likely because GR-Cl and GR-I are isostructural and a solid solution can form between both compounds,[19] i.e., one anion can substitute for the other within the interlayer, without a pronounced effect on the Fe-hydroxide layers. Sorption constants obtained for these experiments (Table S6) are within uncertainties comparable to the results of the no-sulfate model in Figure 2, supporting this hypothesis.

Experiments at higher sulfate concentrations, i.e., the $SO_4^{2-}$ concentration in uptake experiments with 9 g/kg GR-Cl (i.e., ∼20 mmol/L GR-Cl) was higher than that of $Cl^-$ ($SO_4^{2-}/Cl^-$ = ∼2:1), imply a nearly quantitative transformation of GR-Cl to GR-$SO_4$. A model describing the GR-Cl conversion to GR-$SO_4$ was reported in 2020 by Agnel et al.[41] In the series of experiments at high $SO_4^{2-}$ concentration, no iodide sorption could be measured. GR-$SO_4$ has, thus, a very low affinity for iodide sorption. GR-$SO_4$ on the one hand and GR-Cl and GR-I on the other hand are not isostructural and have different organizations of the interlayer (hexagonal vs rhombohedral). Structural changes are likely related to the differences in geometry, charge, and hydration behavior of the interlayer anions (spherical and monovalent for $Cl^-$ and $I^-$ compared to tetrahedral divalent for $SO_4^{2-}$). These differences are the most likely explanation for the missing affinity of GR-$SO_4$ to take up iodide and point toward the possible description of GR-(Cl, I) as a solid solution, where solid mixing is always preferred for isostructural solids.

**X-ray Absorption Spectroscopy.** Iodine K-edge X-ray absorption spectra have been recorded for samples prepared considering various $pH_m$ and ionic strength conditions (Table S5). In the edge region, XANES spectra are comparable for all GR samples (Figure 4), implying that variations of $pH_m$ or ionic strength have no influence on the iodine speciation. The XANES of all GR samples are also similar to that of the $NaI_{(aq)}$ reference compound, indicating the same oxidation state and

Table 1. Quantitative EXAFS Analysis of GR Samples and the $NaI_{(aq)}$ Reference Compound at the Iodine K-edge

| Sample | FT range[a] [Å$^{-1}$] | Fit range[b] [Å] | Shell | $N$ | $d$ [Å] | $\sigma^2$ [Å$^2$] | $\Delta E_0$ [eV] | $R_f$ |
|---|---|---|---|---|---|---|---|---|
| GR-Cl-191 | 2.9−7.5 | 2.25−4.1 | O | 6 | 3.52(2) | 0.015(2) | −1.0 | 0.014 |
| GR-Cl-192 | 2.9−7.5 | 2.25−4.1 | O | 6 | 3.52(3) | 0.012(2) | −1.1 | 0.028 |
| GR-Cl-195 | 2.9−7.5 | 2.25−4.1 | O | 6 | 3.53(2) | 0.020(1) | −0.1 | 0.008 |
| $NaI_{(aq)}$ | 2.9−7.5 | 2.25−4.1 | O | 6 | 3.52(2) | 0.022(1) | −1.3 | 0.004 |

[a]Fourier transformed range. [b]$R + \Delta R$ interval for the fit. $N$ is the coordination number (fixed), $d$ is the interatomic distance, $\sigma^2$ is the mean square displacement (Debye−Waller term), $\Delta E_0$ is the shift in ionization energy with $E_0$ threshold energy taken as the maximum of the first derivative, and $R_f$ is the figure of merit of the fit as reported in ref 44. The numbers in parentheses indicate the uncertainty.

short-range environment (Figure 4). From the analysis of the XANES, it may be concluded that in all GR samples iodide is surrounded by a hydration shell comparable to that of the aqueous anions and shows only weak interaction with the substrate, unaffected by $pH_m$, ionic strength, or iodine concentration.

The iodine K-edge EXAFS spectra of all GR samples are very similar (Figure 4) and also comparable to that of the $NaI_{(aq)}$ reference. This agrees with the inspection of the XANES. Fit results indicate that iodine is surrounded by 6 O atoms at $d$(I−O) = 3.52(2) Å in all samples (Figure 4, Table 1). These results agree with the reported crystallographic data of hydrated iodide anions in water[42,43] and the associated high disorder, as indicated by the relatively large Debye−Waller terms. According to the results, changes of $pH_m$ or ionic strength do not affect the hydration shell made of six water molecules binding iodide via H atoms. Overall, XAS data are consistent with a weak electrostatic interaction with the Fe octahedral sheet, comparable to that reported in earlier studies of iodide uptake by formation of a GR-$Cl_{1-x}I_x$ solid solution.[19]

**Modeling of Iodide Sorption by GR-Cl.** Two models were developed in order to analyze possible uptake mechanisms and to quantitatively describe experimental results. The first approach is based on an ion-exchange uptake mechanism. Figures 1b and 2b show data used for the model adjustments (model/filled squares), which precisely reflect the experimental conditions. A more generic model line is depicted ($c$(GR) = 0.025 mol/kg, fixed initial concentrations) to provide a more general view on the sorption behavior predicted by the model. The best agreement between model and experiment was achieved with log ($k_s$) = log ($K_I$) − log ($K_{Cl}$) = 1.07 − 1.00 = 0.07 (eqs 2−5).

Figure S5 in Supporting Information shows the comparison between modeled and experimental data for the isotherm at a $pH_m$ of 8.5. No significant difference with data at $pH_m$ 7.5 could be found at that higher $pH_m$, which agrees with the absence of pH dependence on the anionic-exchange mechanism. Figure 1 further shows a high level of agreement between the calculated model values and the experimental data at different ionic strengths, thereby also confirming that high $Cl^-$ concentrations impede $I^-$ sorption. According to these results, there is no significant preference for one anion over the other (chloride or iodide) for uptake. These results compare well with previously reported solid solution experiments, where the $Cl^-/I^-$ ratio in the GR interlayer was the same as in the contacting aqueous phase.[19] Data from this study further show that the absence of selective uptake of one of these two anions is also valid at higher ionic strength up to 5 mol/kg (Figure 1). This experimental finding is also well captured by the solid solution model. The best fit model used an almost equal solubility constant for both endmembers (log $K_{SP}$(GR-I) = −79.75; log $K_{SP}$(GR-Cl) = −79.70) and assumed ideal mixing within the solid. The slightly lower solubility of GR-I reflects the slightly higher affinity for iodide incorporation compared to chloride, which is as well reflected in log($k_s$) = 0.07. Accordingly, the predicted solid solution distribution coefficient is close to one ($D$ = 1.1),[45] while experimental $R_d$ values can be recalculated to solid solution distribution coefficients ranging from 0.5 to 1.4. The difference in the solubility products is evident as it reflects the affinity for iodide incorporation. However, considering the uncertainty of the solubility constant of GR-Cl (which is not reported in the literature but is likely quite large), the solubility difference is most likely not significant. In Figure S6 it is shown that this simplistic solid solution model matches the experimental data well and that besides the iodide uptake it also adequately predicts the total solid content. A generic solid solution model curve is presented on top of the experimental data in Figures 1b and 2b. It demonstrates the degree of agreement between the two modeling approaches and the experimental results. Consequently, it may be concluded that the iodide uptake by GR-Cl proceeds through an ion-exchange mechanism, which is equivalent to a solid-mixing process, and that all interlayer anion-exchange sites are available for iodide uptake by GR.[33]

GR-Cl synthesis in the presence of iodide and iodide retention by preformed GR-Cl results in comparable uptake and solid phase composition. These results are consistent with literature observations on other LDH phases that hold the potential for radioiodine uptake. High iodide uptake could be achieved by Mg/Al LDHs,[46] Co−Cr layered hydrotalcite[47] or high Ca-containing phases such as hydrocalumite, C-S-H, and portlandite.[48]

**Implications for Radioactive Waste Disposal.** Steel corrosion in a DGR can lead to the formation of various Fe (hydr)oxide phases (e.g., magnetite, ferrous hydroxychloride, GR, among others), the nature of which being dependent on several parameters such as pH, $E_h$, temperature, or composition of the contacting porewater.[5,49,50] For example, depending on the DGR concept, the $Cl^-$ concentration can vary from low to very high and have a significant impact on the retention of radionuclides by Fe corrosion products. Among them, GR-Cl possesses a permanent layer charge, conferring it the potential to retain anionic species such as iodide. Data show that the iodide uptake also depends on its concentration and the chloride concentration present in the porewater. Indeed, chloride competes with iodide for uptake, and low $R_d$ values can be expected for iodide when $Cl^-$ is present in high concentrations, though the retention of trace amounts of $^{129}I^-$ can still be expected in a DGR near-field. Sulfate and carbonate are other anions typically present in groundwater. The stability of GR-$SO_4$ is higher than that of GR-Cl or GR-I. Furthermore, Refait et al. report the preferential formation of GR-$CO_3$ over GR-$SO_4$ when carbonate and sulfate anions are present simultaneously during the preparation of GR.[51] Thus, the

affinity of GR for $CO_3^{2-}$ uptake is even higher compared to $SO_4^{2-}$. Consequently, it must be assumed that carbonate would outcompete iodide on the exchange sites. Overall, the retention or retardation of iodide by GR in a DGR near-field seems limited and highly dependent on the nature and concentration of anionic species present in the porewater.

Beside the composition of the porewater, the availability of GR is another parameter affecting the extent of iodide retention. For the given geochemical conditions, the amount of immobilized iodide is linked to the amounts of GR present for uptake. Since the stability of mineral phases depends on the prevailing geochemical conditions and given that near-field conditions will evolve with ongoing canister corrosion, conditions can be expected to evolve from favorable to the formation of GR to favorable to the formation of other more thermodynamically stable phases such as magnetite. For example, a pH increase to alkaline conditions[52,53] due to, e.g., the interaction of cementitious materials in the DGR or water reduction, would render GR instable, which then converts into magnetite.[35] Based on the present study, the conversion of GR to magnetite will result in a release of iodide that was immobilized by GR.

This study contributes to elucidate the molecular mechanism of iodide uptake by GR-Cl by combining batch experiments, XAS, and geochemical modeling. Good agreement between experimental data and models could be achieved using either an ion-exchange or a solid solution model, suggesting that hydrated iodide ions substitute at random for chloride within the interlayer, whether in adsorption or in coprecipitation experiments.

## ■ ASSOCIATED CONTENT

### ● Supporting Information

The Supporting Information is available free of charge at https://pubs.acs.org/doi/10.1021/acs.est.3c02041.

Structural characterization of GR and magnetite; list of investigated samples, experimental conditions and results; XAS parameters; and model results (PDF)

## ■ AUTHOR INFORMATION


### Corresponding Authors

**Nicolas Finck** − *Institute for Nuclear Waste Disposal (INE), Karlsruhe Institute of Technology (KIT), 76021 Karlsruhe, Germany;* orcid.org/0000-0002-1940-4051; Phone: +49 (0) 721-6082-4321; Email: nicolas.finck@kit.edu

**Tim Platte** − *Institute for Nuclear Waste Disposal (INE), Karlsruhe Institute of Technology (KIT), 76021 Karlsruhe, Germany;* orcid.org/0000-0001-8584-2298; Email: tim.platte@kit.edu

### Authors

**Frank Heberling** − *Institute for Nuclear Waste Disposal (INE), Karlsruhe Institute of Technology (KIT), 76021 Karlsruhe, Germany;* orcid.org/0000-0002-2650-2071

**Robert Polly** − *Institute for Nuclear Waste Disposal (INE), Karlsruhe Institute of Technology (KIT), 76021 Karlsruhe, Germany*

**Tim Prüssmann** − *Institute for Nuclear Waste Disposal (INE), Karlsruhe Institute of Technology (KIT), 76021 Karlsruhe, Germany;* orcid.org/0000-0002-7903-9199

**Kathy Dardenne** − *Institute for Nuclear Waste Disposal (INE), Karlsruhe Institute of Technology (KIT), 76021 Karlsruhe, Germany*

**Horst Geckeis** − *Institute for Nuclear Waste Disposal (INE), Karlsruhe Institute of Technology (KIT), 76021 Karlsruhe, Germany*

Complete contact information is available at: https://pubs.acs.org/10.1021/acs.est.3c02041


### Author Contributions

The manuscript was written through contributions of all authors.

### Notes

The authors declare no competing financial interest.

## ■ ACKNOWLEDGMENTS


We thank E. Soballa and D. Schild (KIT-INE) for SEM analysis. We also thank the Institute for Beam Physics and Technology (IBPT) for the operation of the storage ring, the Karlsruhe Research Accelerator (KARA). We also thank Grace Castle for proofreading. The authors acknowledge support by the state of Baden-Württemberg through bwHPC and the German Research Foundation (DFG) through Grant no. INST 40/575-1 FUGG (JUSTUS 2 cluster). This work has received financial support from the German Federal Ministry for Economic Affairs and Climate Action (BMWK) through the VESPA 2 (Verhalten langlebiger Spalt- und Aktivierungsprodukte im Nahfeld von Endlagern unterschiedlicher Wirtsgesteine und Möglichkeiten ihrer Rückhaltung 2) project under Contract no. 02 E 11607C.


## ■ REFERENCES


(1) McGill, I. R.; McEnaney, B.; Smith, D. C. Crystal Structure of Green Rust Formed by Corrosion of Cast Iron. *Nature* **1976**, *259* (5540), 200−201.

(2) Stampfl, P. P. Ein Basisches Eisen-II-III-Karbonat in Rost. *Corros. Sci.* **1969**, *9* (3), 185−187.

(3) Butler, G.; Beynon, J. G. The Corrosion of Mild Steel in Boiling Salt Solutions. *Corros. Sci.* **1967**, *7* (7), 385−404.

(4) Usman, M.; Byrne, J. M.; Chaudhary, A.; Orsetti, S.; Hanna, K.; Ruby, C.; Kappler, A.; Haderlein, S. B. Magnetite and Green Rust: Synthesis, Properties, and Environmental Applications of Mixed-Valent Iron Minerals. *Chem. Rev.* **2018**, *118* (7), 3251−3304.

(5) Refait, P.; Abdelmoula, M.; GÉnin, J.-M. R. Mechanisms of Formation and Structure of Green Rust One in Aqueous Corrosion of Iron in the Presence of Chloride Ions. *Corros. Sci.* **1998**, *40* (9), 1547−1560.

(6) King, F. Container Materials for the Storage and Disposal of Nuclear Waste. *CORROSION* **2013**, *69* (10), 986−1011.

(7) King, F.; Hall, D. S.; Keech, P. G. Nature of the Near-Field Environment in a Deep Geological Repository and the Implications for the Corrosion Behaviour of the Container. *Corros. Eng. Sci. Technol.* **2017**, *52* (sup1), 25−30.

(8) Lucchini, J.-F.; Borkowski, M.; Richmann, M. K.; Ballard, S.; Reed, D. T. Solubility of Nd3+ and UO22+ in WIPP Brine as Oxidation-State Invariant Analogs for Plutonium. *J. Alloys Compd.* **2007**, *444*−*445*, 506−511.

(9) Abdelmoula, M.; Trolard, F.; Bourrié, G.; Génin, J. M. R. Evidence for the Fe(II)-Fe(III) Green Rust "Fougerite †" Mineral Occurrence in a Hydromorphic Soil and Its Transformation with Depth. *Hyperfine Interact.* **1998**, *112* (1−4), 235−238.

(10) Trolard, F.; Genin, J.-M.; Abdelmoula, M.; Bourrie, G.; Humbert, B.; Herbillon, A. Identification of a Green Rust Mineral in a Reductomorphic Soil by Mössbauer and Raman Spectroscopies. *Geochim. Cosmochim. Acta* **1997**, *61* (5), 1107−1111.

(11) Kaplan, D. I.; Serne, R. J.; Parker, K. E.; Kutnyakov, I. V. Iodide Sorption to Subsurface Sediments and Illitic Minerals. *Environ. Sci. Technol.* **2000**, *34* (3), 399−405.
(12) SAZARASHI, M.; IKEDA, Y.; SEKI, R.; YOSHIKAWA, H. Adsorption of I - Ions on Minerals for 129 I Waste Management. *J. Nucl. Sci. Technol.* **1994**, *31* (6), 620−622.
(13) Tournassat, C.; Gaucher, E. C.; Fattahi, M.; Grambow, B. On the Mobility and Potential Retention of Iodine in the Callovian-Oxfordian Formation. *Phys. Chem. Earth, Parts A/B/C* **2007**, *32* (8−14), 539−551.
(14) Balsley, S. D.; Brady, P. V.; Krumhansl, J. L.; Anderson, H. L. Anion Scavengers for Low-Level Radioactive Waste Repository Backfills. *J. Soil Contam.* **1998**, *7* (2), 125−141.
(15) Muramatsu, Y.; Uchida, S.; Sriyotha, P.; Sriyotha, K. Some Considerations on the Sorption and Desorption Phenomena of Iodide and Iodate on Soil. *Water. Air. Soil Pollut.* **1990**, *49* (1−2), 125−138.
(16) Ticknor, K. V.; Cho, Y.-H. Interaction of Iodide and Iodate with Granitic Fracture-Filling Minerals. *J. Radioanal. Nucl. Chem. Artic.* **1990**, *140* (1), 75−90.
(17) Fuhrmann, M.; Bajt, S.; Schoonen, M. A. A. Sorption of Iodine on Minerals Investigated by X-Ray Absorption near Edge Structure (XANES) and 125I Tracer Sorption Experiments. *Appl. Geochem.* **1998**, *13* (2), 127−141.
(18) Aimoz, L.; Kulik, D. A.; Wieland, E.; Curti, E.; Lothenbach, B.; Mäder, U. Thermodynamics of AFm-(I2, SO4) Solid Solution and of Its End-Members in Aqueous Media. *Appl. Geochem.* **2012**, *27* (10), 2117−2129.
(19) Platte, T.; Finck, N.; Mangold, S.; Polly, R.; Geckeis, H. Retention of Iodide and Chloride by Formation of a Green Rust Solid Solution GR-Cl 1- x I X : A Multiscale Approach. *Inorg. Chem.* **2021**, *60* (14), 10585−10595.
(20) Vinš, J.; Šubrt, J.; Zapletal, V.; Hanousek, F. Preparation and Properties of Green Rust Type Substances. *Collect. Czechoslov. Chem. Commun.* **1987**, *52* (1), 93−102.
(21) Altmaier, M.; Metz, V.; Neck, V.; Müller, R.; Fanghänel, T. Solid-Liquid Equilibria of Mg(OH)2(Cr) and Mg2(OH)3Cl·4H2O(Cr) in the System Mg-Na-H-OH-Cl-H2O at 25°C. *Geochim. Cosmochim. Acta* **2003**, *67* (19), 3595−3601.
(22) Nedel, S.; Dideriksen, K.; Christiansen, B. C.; Bovet, N.; Stipp, S. L. S. Uptake and Release of Cerium During Fe-Oxide Formation and Transformation in Fe(II) Solutions. *Environ. Sci. Technol.* **2010**, *44* (12), 4493−4498.
(23) Finck, N.; Nedel, S.; Dideriksen, K.; Schlegel, M. L. Trivalent Actinide Uptake by Iron (Hydr)Oxides. *Environ. Sci. Technol.* **2016**, *50* (19), 10428−10436.
(24) Zimina, A.; Dardenne, K.; Denecke, M. A.; Doronkin, D. E.; Huttel, E.; Lichtenberg, H.; Mangold, S.; Pruessmann, T.; Rothe, J.; Spangenberg, T.; Steininger, R.; Vitova, T.; Geckeis, H.; Grunwaldt, J.-D. CAT-ACT—A New Highly Versatile x-Ray Spectroscopy Beamline for Catalysis and Radionuclide Science at the KIT Synchrotron Light Facility ANKA. *Rev. Sci. Instrum.* **2017**, *88* (11), 113113.
(25) Parkhurst, D. L.; Appelo, C. *Description of Input and Examples for PHREEQC Version 3—A Computer Program for Speciation, Batch-Reaction, One-Dimensional Transport, and Inverse Geochemical Calculations*; U.S. Geological Survey Techniques and Methods; U.S. Geological Survey: 2013.
(26) Giffaut, E.; Grivé, M.; Blanc, P.; Vieillard, P.; Colàs, E.; Gailhanou, H.; Gaboreau, S.; Marty, N.; Madé, B.; Duro, L. Andra Thermodynamic Database for Performance Assessment: ThermoChimie. *Appl. Geochem.* **2014**, *49*, 225−236.
(27) Heberling, F.; Klačić, T.; Raiteri, P.; Gale, J. D.; Eng, P. J.; Stubbs, J. E.; Gil-Díaz, T.; Begović, T.; Lützenkirchen, J. Structure and Surface Complexation at the Calcite(104)-Water Interface. *Environ. Sci. Technol.* **2021**, *55* (18), 12403−12413.
(28) Prieto, M. Thermodynamics of Solid Solution-Aqueous Solution Systems. *Rev. Mineral. Geochemistry* **2009**, *70* (1), 47−85.
(29) Chivot, J. *Thermodynamique Des Produits de Corrosion Fonctions Thermodynamiques, Diagrammes de Solubilité, Diagrammes E-Ph Des Systèmes Fe-H2O, Fe-CO2-H2O, Fe-S-H2O, Cr-H2O et Ni-H2O En Fonction de La Temperature*; Collection Sciences & Techniques; Andra: Châtenay-Malabry, 2004.
(30) Génin, J. M. R.; Bourrié, G.; Trolard, F.; Abdelmoula, M.; Jaffrezic, A.; Refait, P.; Maitre, V.; Humbert, B.; Herbillon, A. Thermodynamic Equilibria in Aqueous Suspensions of Synthetic and Natural Fe(II)-Fe(III) Green Rusts: Occurrences of the Mineral in Hydromorphic Soils. *Environ. Sci. Technol.* **1998**, *32* (8), 1058−1068.
(31) Min, J. H.; Baik, M. H.; Lee, J. K.; Jeong, J. T. Sorption of I and Se onto Green Rusts with Different Interlayer Anions, GR(CO 3 2-) AND GR(Cl -). *J. Nucl. Fuel Cycle Waste Technol.* **2013**, *1* (1), 57−63.
(32) Curtius, H.; Kattilparampil, Z. Sorption of Iodine on Mg-Al-Layered Double Hydroxide. *Clay Miner.* **2005**, *40* (4), 455−461.
(33) Nedyalkova, L.; Tits, J.; Renaudin, G.; Wieland, E.; Mäder, U.; Lothenbach, B. Mechanisms and Thermodynamic Modelling of Iodide Sorption on AFm Phases. *J. Colloid Interface Sci.* **2022**, *608*, 683−691.
(34) Morelová, N.; Finck, N.; Lützenkirchen, J.; Schild, D.; Dardenne, K.; Geckeis, H. Sorption of Americium/Europium onto Magnetite under Saline Conditions: Batch Experiments, Surface Complexation Modelling and X-Ray Absorption Spectroscopy Study. *J. Colloid Interface Sci.* **2020**, *561*, 708−718.
(35) Jolivet, J.-P.; Tronc, E.; Chanéac, C. Iron Oxides: From Molecular Clusters to Solid. A Nice Example of Chemical Versatility. *Comptes Rendus Geosci.* **2006**, *338* (6−7), 488−497.
(36) Mączka, E.; Jartych, E.; Kosmulski, M. Isoelectric Points of Fresh and Aged Fe(OH)2. *Colloids Surfaces A Physicochem. Eng. Asp.* **2014**, *441*, 326−330.
(37) Fleet, M. E. The Structure of Magnetite: Symmetry of Cubic Spinels. *J. Solid State Chem.* **1986**, *62* (1), 75−82.
(38) Bernal, J. D. The Oxides and Hydroxides of Iron and Their Structural Inter-Relationships. *Clay Miner.* **1959**, *4* (21), 15−30.
(39) Swanson, H. E.; Tatge, E. *Circular of the Bureau of Standards No. 539 Vol. 1: Standard X-ray Diffraction Powder Patterns*; National Bureau of Standards: 1953; p 43.
(40) Refait, P.; Génin, J. M. R. The Transformation of Chloride-Containing Green Rust One into Sulphated Green Rust Two by Oxidation in Mixed Cl- and SO42- Aqueous Media. *Corros. Sci.* **1994**, *36* (1), 55−65.
(41) Agnel, M. I.; Grangeon, S.; Fauth, F.; Elkaïm, E.; Claret, F.; Roulet, M.; Warmont, F.; Tournassat, C. Mechanistic and Thermodynamic Insights into Anion Exchange by Green Rust. *Environ. Sci. Technol.* **2020**, *54* (2), 851−861.
(42) Fulton, J. L.; Schenter, G. K.; Baer, M. D.; Mundy, C. J.; Dang, L. X.; Balasubramanian, M. Probing the Hydration Structure of Polarizable Halides: A Multiedge XAFS and Molecular Dynamics Study of the Iodide Anion. *J. Phys. Chem. B* **2010**, *114* (40), 12926−12937.
(43) Maeda, M.; Ohtaki, H. An X-Ray Diffraction Study of a Concentrated Aqueous Sodium Iodide Solution. *Bull. Chem. Soc. Jpn.* **1975**, *48* (12), 3755−3756.
(44) Finck, N.; Dardenne, K.; Geckeis, H. Am(III) Coprecipitation with and Adsorption on the Smectite Hectorite. *Chem. Geol.* **2015**, *409*, 12−19.
(45) Heberling, F.; Metz, V.; Böttle, M.; Curti, E.; Geckeis, H. Barite Recrystallization in the Presence of 226Ra and 133Ba. *Geochim. Cosmochim. Acta* **2018**, *232*, 124−139.
(46) Theiss, F. L.; Ayoko, G. A.; Frost, R. L. Sorption of Iodide (I-) from Aqueous Solution Using Mg/Al Layered Double Hydroxides. *Mater. Sci. Eng., C* **2017**, *77*, 1228−1234.
(47) Levitskaia, T. G.; Chatterjee, S.; Arey, B. W.; Campbell, E. L.; Hong, Y.; Kovarik, L.; Peterson, J. M.; Pence, N. K.; Romero, J.; Shutthanandan, V.; Schwenzer, B.; Varga, T. RedOx-Controlled Sorption of Iodine Anions by Hydrotalcite Composites. *RSC Adv.* **2016**, *6* (79), 76042−76055.
(48) Liu, X.; Asai, A.; Sato, T.; Opiso, E.; Otake, T.; Yoneda, T. Mineral Synthesis in Si-Al-Ca Systems and Their Iodide Sorption Capacity under Alkaline Conditions. *Water, Air, Soil Pollut.* **2013**, *224* (3), 1442.

(49) Schlegel, M. L.; Necib, S.; Daumas, S.; Blanc, C.; Foy, E.; Trcera, N.; Romaine, A. Microstructural Characterization of Carbon Steel Corrosion in Clay Borehole Water under Anoxic and Transient Acidic Conditions. *Corros. Sci.* **2016**, *109*, 126−144.
(50) Wang, Z.; Moore, R.; Felmy, A.; Mason, M.; Kukkadapu, R. A Study of the Corrosion Products of Mild Steel in High Ionic Strength Brines. *Waste Manag.* **2001**, *21* (4), 335−341.
(51) Refait, P.; Drissi, S. H.; Pytkiewicz, J.; Génin, J.-M. R. The Anionic Species Competition in Iron Aqueous Corrosion: Role of Various Green Rust Compounds. *Corros. Sci.* **1997**, *39* (9), 1699−1710.
(52) Chaparro, M. C.; Finck, N.; Metz, V.; Geckeis, H. Reactive Transport Modelling of the Long-Term Interaction between Carbon Steel and MX-80 Bentonite at 25 °C. *Minerals* **2021**, *11* (11), 1272.
(53) Bildstein, O.; Trotignon, L.; Perronnet, M.; Jullien, M. Modelling Iron-Clay Interactions in Deep Geological Disposal Conditions. *Phys. Chem. Earth, Parts A/B/C* **2006**, *31* (10−14), 618−625.